Effects of the ion mass ratio on the relativistic Weibel instability

Chang-Mo Ryu and Helen H. Kaang

Department of Physics, POSTECH, Pohang 790-784, Korea

(Received: 28 October 2009 / Accepted: 12 February 2010)

The Weibel instability has received renewed attention for its applicability in various astrophysical and laboratory plasmas. The Weibel instability is a plausible mechanism for the magnetic field generation in the gamma ray burst. It is also considered as the source of the cosmological magnetic field in the early universe. This instability also seems to play an important role in a high-intensity laser produced plasma. In this paper, we investigate the ion mass effect on the relativistic Weibel instability by using a particle-in-cell simulation technique, considering two different ion-to-electron mass ratios. The study extends to the nonlinear physics regime. It is found that when the ion-to-electron mass is smaller, the magnetic field energy grows stronger and is more quickly damped, manifesting clearer inverse cascade process following the quasilinear saturation stage. We ascribe this mass effect to the increased electrostatic fluctuation associated with the ion acoustic wave by the enhanced ion mobility.

Keywords: Weibel instability, dynamo mechanism, magnetic field amplification, Particle-in-cell simulation, ion acoustic wave

1. Introduction

Mechanisms of magnetic field generation in plasmas have been of great interest since it has been realized that the magnetic field plays a crucial role in determining the physical properties of various plasmas. Amplification of the magnetic field in a highly conducting medium has been observed not only in astrophysical bodies such as the Earth, the Sun, galaxies, interstellar media, and even in black holes [1, 2, 3, 4, 5, 6, 7], but also in many laboratory plasmas such as the laser evaporated plasma [8, 9], z-pinch [10], reversed field pinch [11, 12], and field reversed configuration [13, 14, 15]. A variety of interesting physical phenomena are found to occur via the interplay between the magnetic field and these plasmas. However, the processes leading to the large scale magnetic fields are largely unknown.

The Weibel instability has recently drawn attention for its possibility to occur in various astrophysical situations. Medvedev and Loeb suggest that the Weibel instability can be a candidate mechanism for generating magnetic fields in the gamma ray burst [16, 17]. Schlickeiser proposes that the Weibel instability might be responsible for the generation of cosmological magnetic fields in the early universe [18]. The role of the Weibel instability in generating large scale cosmic magnetic fields might also be relevant in dark energy [19]. Plasmas in these astrophysical and cosmic bodies, as well as laser plasmas where generation of strong magnetic fields are often observed are highly energetic. As a consequence, the discussion of the Weibel instability in the energetic plasma systems requires a relativistic treatment [20, 21, 22, 23, 24].

The Weibel instability is excited by the localized charged particle motions. The classical study of the Weibel instability has focused mainly on the electrons with an assumption that the ions are immobile [25]. Of many studies into the Weibel instability, only a few on the electron-positron plasmas in gamma ray bursts have dealt with the ion effects, and the ion effects on the Weibel instability have been neglected in general. Even in the case that the ion effects are included, they are merely limited to satisfying the charge neutrality condition. However, with better understanding, realization of the importance of the ion effects starts to emerge. For instance, Medvedev and Loeb have shown that the magnetic field strengths shown in previous simulations are too small compared to actual observations, and thus that the ion effects may have to be considered [16]. In the nonlinear regime where strong coupling to various modes take place, ion effects might be important.

In the present paper, we investigate the ion-to-electron mass ratio effects on the Weibel instability which is driven by temperature anisotropy in a relativistic regime, by employing a one-dimensional PIC(Particle-in-cell) simulation method. We consider two different cases of ion-to-electron mass ratios.

The organization of the paper is as follows: In Sec. 2 the simulation conditions are described. Sec. 3, and Sec. 4 presents the simulation results, and Sec. 5 presents conclusions.

author's e-mail: ryu201@postech.ac.kr

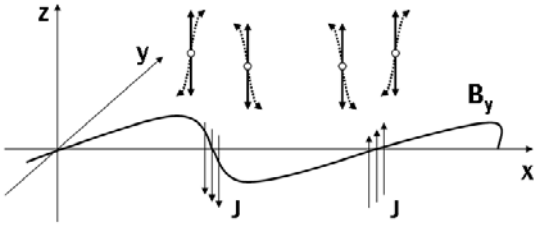

Fig. 1 Schematic of the Weibel instability.

2. Simulation Conditions

The initial electron distribution is taken as a fully relativistic bi-Maxwellian distribution, which is given in Ref. [21],

$$f = \frac{\alpha_\perp \, e^{-\alpha_\perp(\gamma-\gamma_\parallel)-\alpha_\parallel\gamma_\parallel}}{4\pi(mc)^3\, K_2(\alpha_\parallel)\, A},$$
$$A = 1+\left(\frac{\alpha_\parallel}{\alpha_\perp}-1\right)\frac{K_1(\alpha_\parallel)}{\alpha_\parallel\, K_2(\alpha_\parallel)}, \qquad (1)$$

where $\gamma = (1 + p^2/m^2c^2 + p_\parallel^2/m^2c^2)^{1/2}$ is the relativistic Lorentz factor with m and c being the electron rest mass and the speed of light *in vacuo*, respectively. The direction of the wave propagation is taken as the x axis, and the parallel and perpendicular directions are defined along and perpendicular to it, respectively. Then, we define $\gamma_\parallel = (1 + p_\parallel^2/m^2c^2)^{1/2}$. $K_n(x)$ is the modified Bessel function of the second kind of order n. Dimensionless parameters $\alpha_\parallel = mc^2/T_\parallel$ and $\alpha_\perp = mc^2/T_\perp$ characterize the plasma temperature defined along the parallel and perpendicular directions to the wave propagation direction, respectively.

The computer code used in this study is a relativistic electromagnetic particle-in-cell(PIC) code with one spatial and three velocity dimensions (1D3V). Particles are initially loaded according to the bi-Maxwellian distribution function described above. The number of grids N_x is 4096, and for each cell, 4000 particles are allocated. The plasma density is initially uniform. A periodic boundary condition is used at both ends. The grid size is given by $\Delta x = 0.1c/\omega_{pe}$ and the time step by $\Delta t = 0.001/\omega_{pe}$, where $\omega_{pe} = (n_e e^2/\epsilon_0 m)^{1/2}$ is the plasma frequency. Here, ϵ_0 is the vacuum permittivity. We take ω_{pe}^{-1} as the unit time and the electron skin depth c/ω_{pe} as the unit length. We considered two cases of the ion-electron plasma with mass ratios of $M/m = 1833$ and $M/m = 10$. When the mass ratio is small, the ion mobility increases, and thus we expect that the ion effects would be pronounced. The ions are taken to have the same temperature as the electrons.

The simulation was performed until $400\omega_{pe}t$. The Weibel instability occurs when the perpendicular temperature is higher than the parallel temperature. The schematic of its operating mechanism is illustrated in Fig.1. The simulations are performed for various perpendicular thermal anisotropic parameters, and among these, we have chosen $\alpha_\perp = 5$ and $\alpha_\parallel = 30$ as the representative parameters.

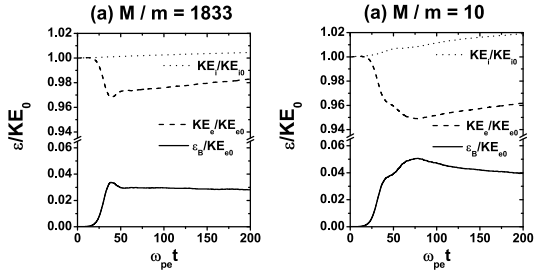

Fig. 2 Evolution of the energy. Magnetic field energy(solid line) and kinetic energy(dashed line) of the electrons are plotted together with the kinetic energy (dotted line) of the ions for (a) M/m = 1833 and (b) M/m =10, respectively.

3. Growth of the Magnetic Field Energy

In Figure 2, time evolution of the magnetic field energy and the kinetic energy of the electrons are shown together with the kinetic energy of the ions. The first two energies are normalized by the initial electron thermal energy and the ion kinetic energy is normalized by the initial ion energy. The increase of the magnetic field energy is about the same as that of the decrease of electron energy. Although not shown, the electrostatic field energy does not show appreciable change, indicating that the unstable mode is the electromagnetic one. However, in the case of $M/m = 10$, the ion kinetic energy is shown to continuously increase in time.

In Figure 2, it is shown that the increase of the magnetic field energy is accompanied by a decrease in the electron thermal energy of equal magnitude for the time up to $\omega_{pe}t \sim 40$. Since the ions are much heavier than electrons, the ion effects can appear only in a later phase, and, as a result, the simulations for the two different ion masses show almost the same behavior in the initial phase when the Weibel instability grows linearly. This observation is in agreement with the theoretical expectation.

After passing the linear stage, the plasmas enter a quasilinear and then a nonlinear state. For $M/m = 1833$, the B field energy first undergoes a small overshoot before settling down to a quasi-steady asymptotic state, until the end of the simulation. The saturated B field energy is at about 3% of the initial kinetic energy of the electrons. The B field energy for a smaller ion mass increases up to about 5% of the total initial kinetic energy of the electrons taking longer time $\omega_{pe}t \sim 80$. As the nonlinear effect involving the ions sets in, the electron distribution also shows satu-

ration.

With the assumption that the ions are immobile, the solution of the Vlasov equation for the electrons alone can give rise to the dispersion relation for the Weibel instability as [24],

$$\begin{aligned}\frac{c^2k^2}{\omega_p^2} &= \frac{\alpha_\perp^2\alpha_\parallel}{\alpha_\parallel K_2(\alpha_\parallel)+\Delta K_1(\alpha_\parallel)} \\ &\times\left\{\frac{\Delta}{\alpha_\perp^2}\left(\frac{K_0(\alpha_\parallel)}{\alpha_\perp}+K_1(\alpha_\parallel)\right)\right. \\ &-\frac{\Gamma}{ck}\int_0^\infty\frac{d\tau}{\xi_\perp^2}\left[3\Delta\frac{K_0(\alpha_\parallel)}{\xi_\perp^2}\right. \\ &+\left(3\Delta\frac{\xi_\parallel}{\xi_\perp}+\frac{\xi_\parallel}{\xi_\perp}-\frac{\alpha_\parallel}{\alpha_\perp}\right)\frac{K_1(\zeta)}{\zeta} \\ &\left.\left.+\,\xi_\parallel^2\frac{\alpha_\parallel}{\alpha_\perp}\frac{K_2(\zeta)}{\zeta^2}\right]\right\}, \qquad (2)\end{aligned}$$

where τ is the normalized time, and

$$\begin{aligned}\Delta &= \frac{\alpha_\parallel}{\alpha_\perp}-1, \\ \xi_\perp &= \alpha_\perp+\frac{\Gamma}{ck}\tau, \\ \xi_\parallel &= \alpha_\parallel+\frac{\Gamma}{ck}\tau, \\ \zeta &= \sqrt{\xi_\parallel^2+\tau^2}.\end{aligned}$$

Figure 3 shows the growth rate Γ/ω_pe obtained from the solution for Eq. (2) with $\alpha_\perp = 5$, $\alpha_\parallel = 30$. In this graph, Γ/ω_pe has a maximum at $kc/\omega_{pe} \approx 0.916$ with the value $0.151\omega_{pe}$, and thus, the most unstable mode appears at $kc/\omega_{pe} = 0.916$.

Simulation results are shown in Fig. 4 for the two different mass ratios. A few modes growing most rapidly are plotted. The vertical scale is on a logarithmic amplitude scale. It can be seen that the slopes of the mode amplitudes are about the same, indicating that the linear growth rates are almost the same, but the mode with $kc/\omega_{pe} = 0.92$ has the highest growth rate in agreement with the theoretical prediction. Therefore, we select the mode with $kc/\omega_{pe} = 0.92$ in the PIC simulation as the representative case of the study. By estimating the growth rate from the linear fitting, we get $\Gamma = 0.144\omega_{pe}$ for $M/m = 1833$, $0.137\omega_{pe}$ for $M/m = 10$ [Fig. 5]. The growth rate estimated from the simulation shows an excellent agreement with the one obtained from Eq. (2), which considered the electrons alone. The result that almost the same growth rates are obtained for two different ion-to-electron mass ratios, in agreement with the theoretical prediction confirms that there is no effect of ions on the Weibel instability in the early, linearly growing phase.

It is shown in case of the smaller ion-to-electron mass ratio that the increase of the magnetic field occurs simultaneously with the reduction of the ion temperature anisotropy. Time evolutions of the electron and ion momentum distribution are plotted in Figs. 6 and 7. The initial distribution (shown in Figs.6 and 7 (a) and (c)) has an elliptical shape in the $p_x - p_y$ momentum space. Figures 6 and 7 (b) show that the distribution broadens in time in both the x and y directions. There is no difference in the electron distributions for the two different mass ratios. However, the difference in the ion distribution is noticeable. Unlike the case of $M/m = 1833$ where there is no change, in the case of $M/m = 10$, ion distribution becomes broadened to a rectangular shape. The ion momentum values do not go beyond the boundary values, similarly to the case of the electrons. The rectangular boundary remains the same after the particle distributions are settled, and the magnetic field energy has stopped its increase.

On the other hand, as the ion temperature anisotropy is reduced, the ion thermal energy does not convert into the magnetic field energy, in contrast to the fact that the electron thermal energy converts to

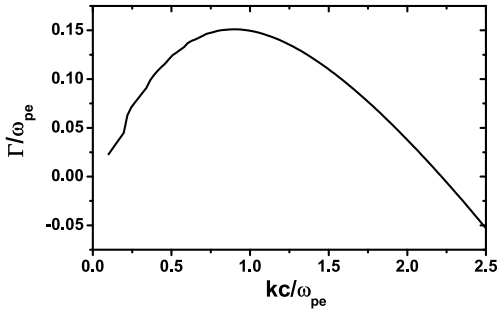

Fig. 3 Linear growth rate obtained from Eq. (2) vs. wave number for $\alpha_\perp = 5$ and $\alpha_\parallel = 30$.

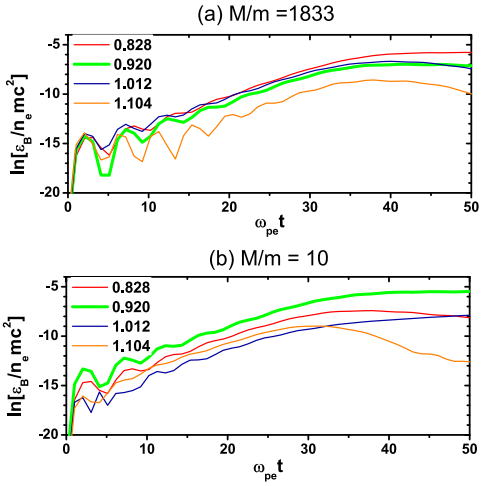

Fig. 4 (Color online) Time evolution of several different modes in the linear regime, for (a) $M/m = 1833$ and (b) $M/m = 10$.

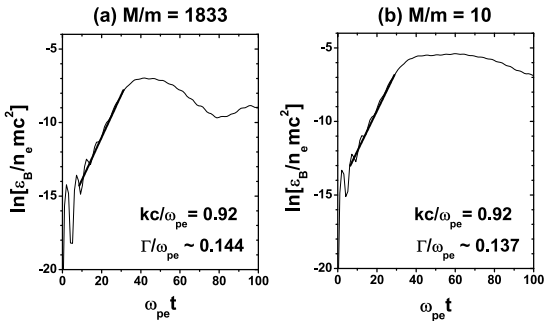

Fig. 5 Time evolution of the mode with $kc/\omega_{pe} = 0.920$ for (a) $M/m = 1833$ and (b) $M/m = 10$.

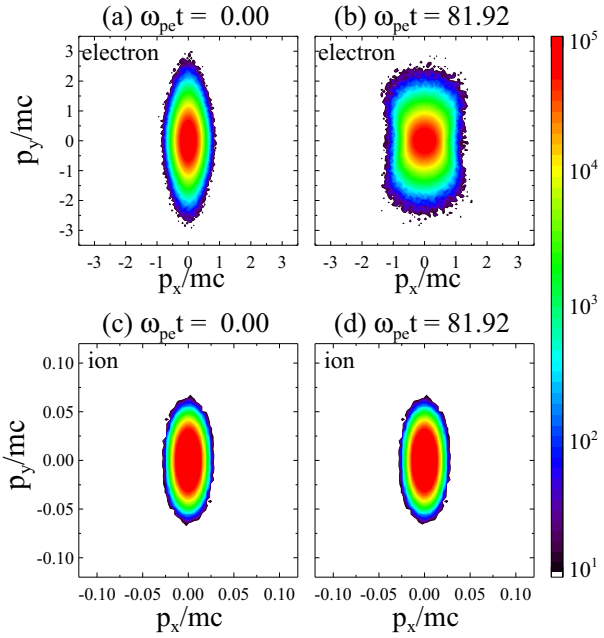

Fig. 6 (Color online)Electron and ion distributions in the momentum space at different times for M/m =1833.

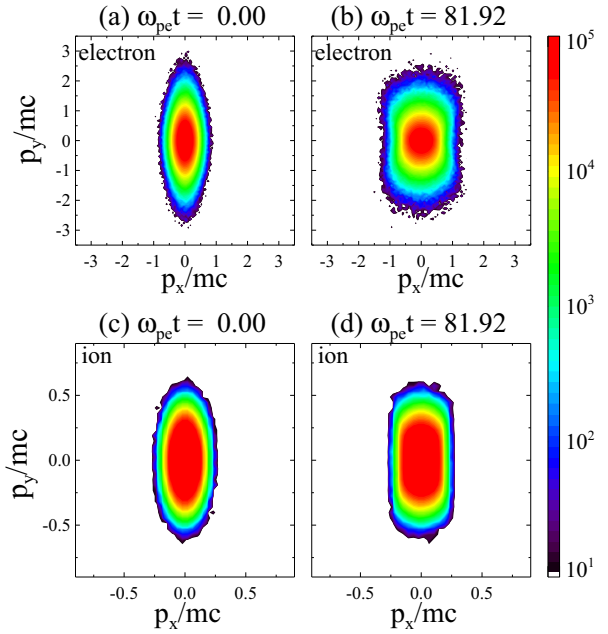

Fig. 7 (Color online)Electron and ion distributions in the momentum space at different times for M/m =10.

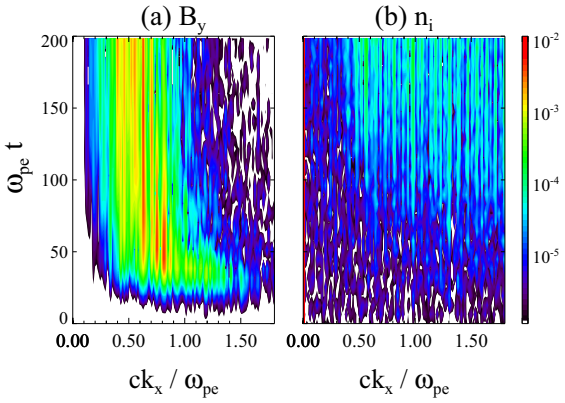

Fig. 8 (Color online) Power spectra of (a) magnetic field B_y and (b)ion density n_i for M/m=1833.

the magnetic field energy. It is shown that as the ion distribution become isotropic, the thermal energy increases, whereas as the electron distribution becomes more isotropic, more magnetic fields are generated [Fig. 2(b)]. It can also be seen that for $M/m = 10$, around $50 \sim 80\omega_{pe}$ the electron thermal energy is reduced and the magnetic field energy increases by the same amount. The increase of the electron isotropy for a lower ion-to-electron mass ratio plasma has also been observed in other PIC simulations [26].

4. Nonlinear regime

After the linear phase and passing the quasilinear phase, merging of small-scale structures of fluctuations into a larger scale one shows up revealing an inverse cascade process. Figs. 8 and 9 show the time evolution of the B_y and n_i spectra. The two spectra are normalized by the electron rest energy. In the early linear growth phase, the strongest wave appears at $kc/\omega_{pe} \sim 0.9$ as mentioned before. As the time evolves, the k numbers of the dominant waves become smaller. The inverse cascade features of B field and ion density show significant difference for the two different mass ratios. In case of the magnetic field, the inverse cascade is independent of the ion-to-electron mass ratio, but for $M/m = 10$ merging of modes occurs more actively. The ion density fluctuation shows a manifest difference for the two different mass ratios.

Figure 10 shows the plot of the electrostatic fluctuations of $\omega - k$ spectrum. We have drawn this figure to identify the modes in Fig.9(b)of n_i fluctuation. The red line corresponds to the dispersion curve for the IA(Ion Acoustic) wave. On this curve, the existence of the IA wave can be identified by a strong

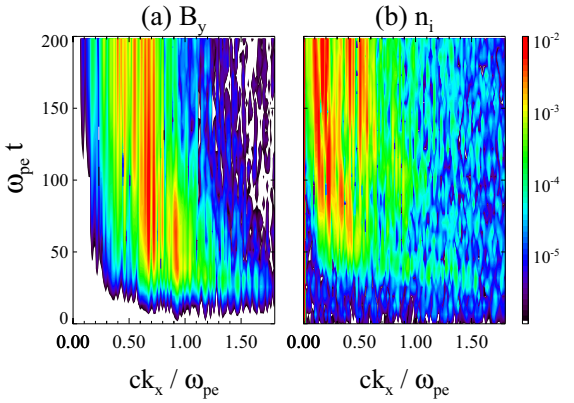

Fig. 9 (Color online) Power spectra of (a) magnetic field B_y and (b)ion density n_i for M/m=10.

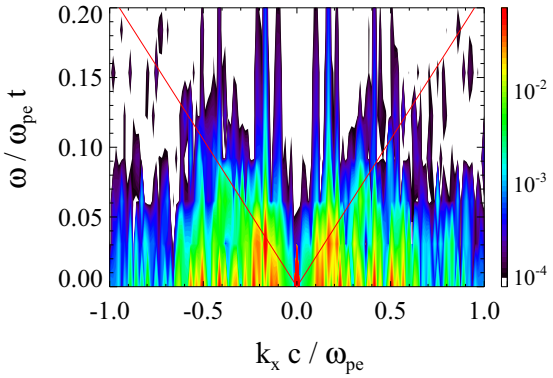

Fig. 10(Color online) $\omega - k$ spectrum of the ion density n_i for M/m=10 during the time $0.0 \sim 204.8\omega_{pe}t$. The red line is the dispersion curve for the ion-acoustic wave.

intensity area around $k_x c/\omega_{pe}t \sim 0.2$. Below this IA mode, many fluctuations are shown to exist near zero frequency.

The inverse cascade process seems to involve an electrostatic mode induced by the ion motion via the wave-wave coupling. The result that the electrostatic fluctuation shows an inverse cascade pattern similar to that of the magnetic field, and that n_i fluctuation intensity increases during this process indicate they are not independent of each other. Electrostatic modes like the IA wave can participate in the inverse cascade process of the Weibel instability.

5. Discussion and conclusions

Large scale magnetic fields are present in many astrophysical and laboratory plasmas, playing important roles in many interesting plasma dynamics. Processes leading to these large scale magnetic fields in the universe or laboratory plasmas, the so-called dynamo mechanism, are not yet clear.

The Weibel instability is one of those candidate mechanisms to explain such a large scale magnetic field in a plasma. The interesting aspect of the Weibel instability is that excess energy stored in the anisotropic distribution of the electrons in a plasma could be released as magnetic field energy by the instability, producing the magnetic field in the electrostatic environment of the null magnetic field. This instability could provide a seed magnetic field such as the primordial field in the early universe.

Classical study of the Weibel instability has mainly focused on the electron motion with an assumption that ions are immobile. In the nonlinear regime where strong coupling to various modes could take place, this assumption may not be valid. We have investigated the ion mobility effect on the Weibel instability by using a 1D PIC simulation. In the early growth phase, when the ions do not have time to contribute, the magnetic field energy increases exponentially, independent of the mass ratio. However, the ion effect becomes evident in the nonlinear regime. When the mass ratio is small compared to the realistic one, the maximum magnetic field energy attained becomes much higher. In this case, the ion distribution expands as the electron distribution does. When this expansion stops, the magnetic field energy does not increase further. For a small mass ratio case, the ion thermal energy is shown to increase continuously.

The inverse cascade process is clearly seen for the magnetic field energy in both cases. In the inverse cascade process, coupling to the electrostatic fluctuations like the ion acoustic mode is strongly indicated.

This work was supported by the grants from BK21 and by the Korea Science and Engineering Foundation (KOSEF) grants R11-2008-072-01003-0 and R01-2003-000-10402-0 from the Korean Ministry of Education, Science and Technology (MEST).

[1] E. N. Parker, Astrophys. J. **122**, 293 (1955).
[2] A. M. Soward, Phil. Trans. Roy. Soc. A **272**, 431 (1972).
[3] F. Krause and K. H. Rädler, *Mean-Field Magnetohydrodynamics* (Pergamon, Oxford, 1980).
[4] H. K. Moffat, *Magnetic Field Generation in Electrically Conducting Fluids* (Cambridge University Press, Cambridge, 1978).
[5] F. Krause, *The Cosmic Dynamo: From $t = -\infty$ to Cowling's theorem. A review on history*, in The Cosmic Dynamo, edited by F. Krause, K. H. Rädler, and G. Rüdiger (Kluwer Academic, Dordrecht, 1993), pp. 487-499.
[6] T.-Y. Lee, and C.-M. Ryu, Phys. Plasmas **11**, 5462 (2004).
[7] T.-Y. Lee, and C.-M. Ryu, J. Phys. D **40**, 5912 (2007).
[8] J. A. Stamper and B. H. Ripin, Phys. Rev. Lett., **34**, 138 (1975).
[9] A. Raven, O. Willi, and M. G.Haines, Phys. Rev. Lett., **35**, 1336 (1975).

[10] F. J. Wessel, F. S. Felber, N. C. Wild, and H. U. Rahman, Appl. Phys. Lett. **83**, 48 (1986).
[11] H. A. Bodin and N. A. Mewton, Nuclear Fusion, **20**, 1255 (1980).
[12] H. Ji, S. C. Prager, A. F. Almagri, J. S. Sarff, Y. Yagi, Y. Hirano, K. Hattori, and H. Toyama, Phys. Plasmas **3**, 1935 (1996); H. Ji and S. C. Prager, Magnetohydrodynamics **38**, 191 (2002).
[13] M. Tuszewki, Nucl. Fusion **28**, 2033 (1988).
[14] N. Rostoker, M. Bindevauer, and H. Monkhorst, Science **278**, 1419 (1997).
[15] A. Hassam, R.M. Kulsrud, R.J. Goldstone, H. Ji, and M. Yamada, Phys. Rev. Lett **83**, 2969 (1999);
[16] M. V. Medvedev and A. Loeb, Astrophys. J. **526**, 697 (1999).
[17] J. Pruet, K. Abazaijian, and G. M. Fuller, Phys. Rev. D **64**, 063002 (2001).
[18] R. Schlickeiser, Plasma Phys. Control. Fusion **47**, A205 (2005).
[19] I. Contopoulos and S. Basilakos, Astron. Astrophys. **471**, 59 (2007).
[20] P. H. Yoon and R. C. Davidson, Phys. Rev. A **35**, 2718 (1987).
[21] P. H. Yoon, Phys. Fluids B **1**, 1336 (1989).
[22] T.-Y. B. Yang, Y. Gallant, J. Arons, and A. B. Langdon, Phys. Fluids B **5**, 3369 (1993).
[23] R. Schlickeiser, Phys. Plasmas **11**, 5532 (2004).
[24] H. H. Kaang, C.-M. Ryu, and P. H. Yoon, Phys. Plasmas **16**, 82103 (2009).
[25] E. S. Weibel, Phy. Rev. Lett. **2**, 83 (1959).
[26] A. Spitkovsky, Astrophys. J. **673**, L39 (2008).